

# Flexible resistive switching device based on poly(3,4-ethylenedioxythiophene):poly(styrene sulfonate) (PEDOT:PSS)/poly(4-vinylphenol) (PVP) composite and methyl red heterojunction

Gul Hassan<sup>1</sup> · Shawkat Ali<sup>1</sup> · Jinho Bae<sup>1</sup> · Chong Hyun Lee<sup>1</sup>

Received: 2 August 2016 / Accepted: 7 March 2017 / Published online: 17 March 2017  
© Springer-Verlag Berlin Heidelberg 2017

**Abstract** To obtain a desired performance of non-volatile memory applications, heterojunction-based resistive switching devices have tremendous attractions. In this paper, we demonstrate resistive switching characteristics for heterojunction of poly(3,4-ethylenedioxythiophene):poly(styrene sulfonate) (PEDOT:PSS)/poly(4-vinylphenol) (PVP) composite and methyl red sandwiched in between bottom and top silver (Ag) electrodes. The proposed heterojunction layers are fabricated through spin coater at 3000 rpm for 60 s each, and the Ag electrodes are deposited through a commercialized inkjet printer DMP-3000 on polyethyleneterephthalate (PET) substrate. To verify the proposed device, the resistive switching on dual polarity voltage of  $\pm 10.2$  V is measured over more than 500 endurance cycles. The paper also presents an  $R_{\text{off}}/R_{\text{on}}$  ratio which can adjust through an active layer's area and a blending ratio of the PEDOT:PSS and PVP. By applying the area of  $100 \mu\text{m}^2$  and the blending ratio of 3:1, we achieve the higher  $R_{\text{off}}/R_{\text{on}}$  ratio of 121, and its high resistance state (HRS) and low resistance state (LRS) are observed as 3000 k $\Omega$  and 24.7 k $\Omega$ , respectively. To maintain a long retention time, the device is encapsulated with PDMS, which changes a little variations of 52  $\Omega$  for HRS 498  $\Omega$  for LRS over 60 days. For the flexible realization to be utilized in wearable applications, it can be easily applied on a plastic substrate using printed technologies.

## 1 Introduction

Resistive switching characteristics were discovered in 1960, and Leon Chua mathematically introduced memristor in 1971 [1]. The memristor is two-terminal passive element that directly relates the charge flow with flux in electrical circuits [2]. As the memristor has characteristics of an analog switch by nature, many researchers have been studying a memristor device with the resistive switching to substitute for transistors. It can be easily realized through the flexible and low-temperature processing techniques in contrast with a transistor. Hence, organic materials for the printed electronics become interested due to its solution based processibility, structure simplicity, low-temperature processing, environmentally friendly, and mechanical flexibility [19–23]. Especially, to improve characteristics such as switching speed, retention time, current density,  $R_{\text{off}}/R_{\text{on}}$  ratio, and stability of these resistive switching devices, researchers are exploring how to design an active layer [3–7]. Due to these characteristics depend on the materials used for the active layer and electrodes, the investigation of materials to be used with realization of the memristor is very important [7–9]. Several memristors can be fabricated using a single insulator for the active layer such as metal sulfide [10], metal oxide [11], nonmetal oxide [12], phase change materials [13], and composite materials [14] based on redox reaction, ion migration, or electrode metallization, whereas several resistive switching devices can be realized through heterojunction of two layers based on defects and ion migration [15]. In the literatures, bipolar resistive switching devices using  $\text{WO}_x/\text{AlO}_y$  heterojunction [16] and  $\text{CuO}/\text{CuO}_2$  heterojunction [17] were demonstrated. Since these results need many improvements in aspect of stability,  $R_{\text{off}}/R_{\text{on}}$  ratio, and retention time, many researchers are exploring new materials to improve the performance

✉ Jinho Bae  
baejh@jejunu.ac.kr

<sup>1</sup> Department of Ocean System Engineering, College of Ocean Science, Jeju National University, 102 Jejudaehakro, Jeju-si, Jeju Special Self-Governing Province 63243, Republic of Korea

of heterojunction devices. P-type and n-type materials were applied as switching devices in semiconductor industry and these p–n heterojunction materials are known in recent year to enable developing of novel multifunctional devices with resistive switching [18].

To explore a new heterojunction resistive switching device, in this paper, the resistive switching device based on poly(3,4-ethylenedioxythiophene):poly(styrene sulfonate) (PEDOT:PSS)/poly(4-vinylphenol) (PVP) composite and methyl red heterojunction is proposed. The  $R_{\text{off}}/R_{\text{on}}$  ratio of the proposed device can be designed through its active layer's area and a blending ratio for the PEDOT:PSS and PVP composite. The proposed device is operating as resistive switching on dual polarity voltage of  $\pm 10.2$  V. To support the design of the device, we have demonstrated the variations of the  $R_{\text{off}}/R_{\text{on}}$  ratio along the variation of the active layer's area and the blending ratio for the PEDOT:PSS/PVP composite, respectively. Especially, it means that the resistance is increased by blending PVP in PEDOT:PSS and the active layer's area, which play an important role in the  $R_{\text{off}}/R_{\text{on}}$  ratio of the device. By applying both the area of  $100 \mu\text{m}^2$  and the blending ratio of 3:1 for the device, we obtained the higher  $R_{\text{off}}/R_{\text{on}}$  ratio of 121. Its high resistance state (HRS) and low resistance state (LRS) are observed as  $3000 \text{ k}\Omega$  and  $24.7 \text{ k}\Omega$ , respectively. The proposed device is composed of Ag bottom electrode/PEDOT:PSS/PVP composite and methyl red sandwiched layers/Ag top electrode on PET substrate. It was fabricated through all printing techniques, where the Ag electrodes and the heterojunction layers were fabricated through commercialized Fujifilm Dimatix Materials Printer DMP-3000 and spin coater, respectively. The deposited layers of the fabricated device are characterized through field emission electron microscopy (FE-SEM) for surface morphology. It is also analyzed for electrical characteristics using Agilent Semiconductor Device Analyzer (B1500A). For the mechanical characterization of the device, the flexibility test was conducted using homemade bending machine. These results could be a good basis for development of heterojunction resistive switching in the printed electronics.

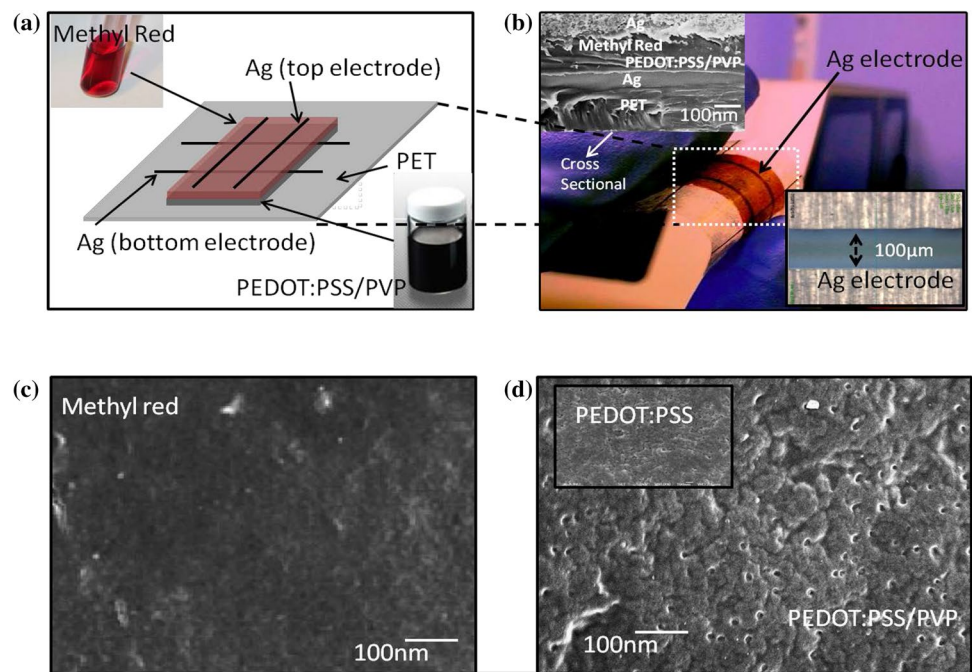
## 2 Materials and fabrications

To fabricate the proposed device, a  $100 \mu\text{m}$  PET substrate, PEDOT:PSS paste organon EL-P5010 with 3 wt% solid content, methyl red with molecular formula  $\text{C}_{15}\text{H}_{15}\text{N}_3\text{O}_2$  in powder form, PVP average  $M_w \sim 25,000$ , and Ag ink 50 wt% dispersion in tripropylene glycol mono methyl ether were prepared from Sigma-Aldrich, South Korea. The non-polymeric organic compound methyl red is an organic semiconductor in the form of dark red crystalline

powder. The PEDOT:PSS is a polymer mixture of two ionomers. The one component in this mixture is made up of sodium polystyrene sulfonate and carries a negative charge. The other component PEDOT:PSS is a conjugated polymer, which carries positive charge and is based on polythiophene. For the heterojunction films, the inks were prepared as: 10 wt% methyl red in benzene and stirred for 2 h at room temperature. PEDOT:PSS solvent-based paste was diluted by 10 wt% in de-ionized water. 0.25 g of PVP was added to the 5 ml of distilled water and the solution was stirred for 2 h. The PEDOT:PSS and the PVP materials were blended with several ratios of 3:0, 3:1, 3:2, and 3:3 by bath sonication for 1 h. The Ag ink was used as purchased without any further processing, and its specifications are solid content of 30–35%, viscosity of 10–17 cPs, surface tension of 35–38, triethylene glycol monomethyl ether (TGME) is used as solvent, resistivity of 11–12  $\mu\Omega/\text{cm}$ , and thickness of Ag electrode of 100–110 nm.

Prior to begin with fabrication, the substrate was rinsed with ethanol and few dips in distilled water to remove the ethanol. Afterward, the substrate was treated UV ozone for 1 min. As the layout diagram shown in Fig. 1a, the device is fabricated. Here, the bottom electrodes were printed with the commercial drop-on-demand Dimatix DMP-3000 material printer with a 10 pL cartridge drop size on the PET substrate and cured at  $70^\circ\text{C}$  for 30 min. We have fabricated Ag electrodes with 100–350  $\mu\text{m}$  width to analyze the performance of devices along active area size. The PEDOT:PSS/PVP composite layer was deposited through the spin coater at 3000 rpm for 60 s and cured for 90 min at  $100^\circ\text{C}$ , and similarly, methyl red layer was deposited by using the spin coater with same parameters and cured at  $100^\circ\text{C}$  for 90 min. At the end, top electrodes were deposited through inkjet printer and cured at  $70^\circ\text{C}$  on the hot platen of the inkjet printer for 60 min. The proposed memory device was fabricated, as shown in Fig. 1b, and the upper inset shows cross-sectional SEM image view of the device at cross point showing the Ag bottom electrode, active heterojunction layers, and the Ag top electrode on PET substrate, where the lower right inset shows the Ag electrode line from top view. The active layers of the heterojunction device were analyzed with FE-SEM Jeol JSM-7600F for surface morphology characterization. Figure 1c shows the SEM image of the methyl red layer on 100 nm scale with  $\times 50,000$  zoom, which shows that the film is uniformly deposited and sintered properly without cracks and pores. Similarly, the PEDOT:PSS/PVP layer was analyzed on 100 nm scale, as shown in Fig. 1d, with the same  $\times 50,000$  zoom where the upper inset shows the SEM image of the PEDOT:PSS without the PVP blending.

**Fig. 1** **a** Device structure. **b** Zoomed image of the proposed device, where the *left top inset* is the cross-sectional view at the cross point with 100 nm scale bar and the *right bottom inset* is the electrode zoomed image with average width of 100  $\mu\text{m}$ . **c** FE-SEM image of the methyl red layer with scale bar of 100 nm. **d** FE-SEM image of the PEDOT:PSS/PVP composite layer (The *left top inset* is the SEM image of 100 nm for the PEDOT:PSS)

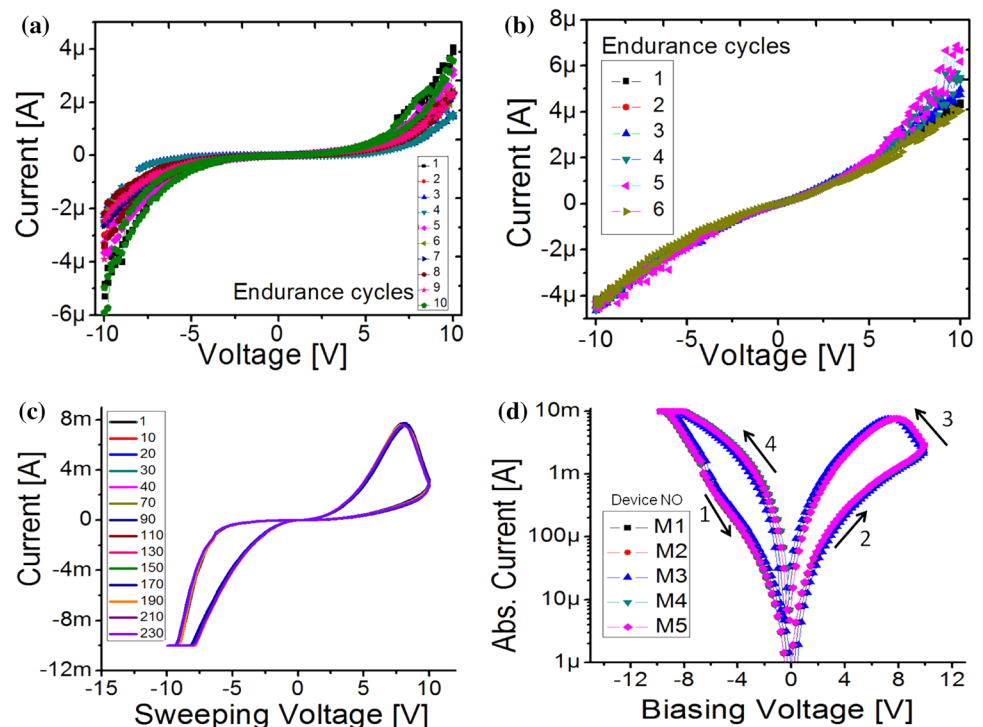


### 3 Characterizations

Agilent B1500A Semiconductor Device Analyzer is used for the electrical characterizations of the resistive switching device. To show sure the resistive switching of the proposed device by the heterojunction of two films, we fabricated a single layered film of each material, which

analyzed for the resistive switching, as shown in Fig. 2a and b. Each device was placed in the probe station and probed were connected across the device as bottom and top electrodes. A dual polarity voltage sweep from  $-10$  to  $10$  V was applied across the methyl red-based device, as shown in Fig. 2a. From these curves, we observed that there was no memory window in the methyl red film. Similarly, the

**Fig. 2** **I-V** curves of the various device fabricated by the various material combinations, **a** **I-V** curve of a single layer methyl red, **b** **I-V** curve of a single layer PEDOT:PSS, **c** **I-V** curve of the PEDOT:PSS and methyl red heterojunction, and **d** absolute current analysis on semi-log scale and fabrication consistency



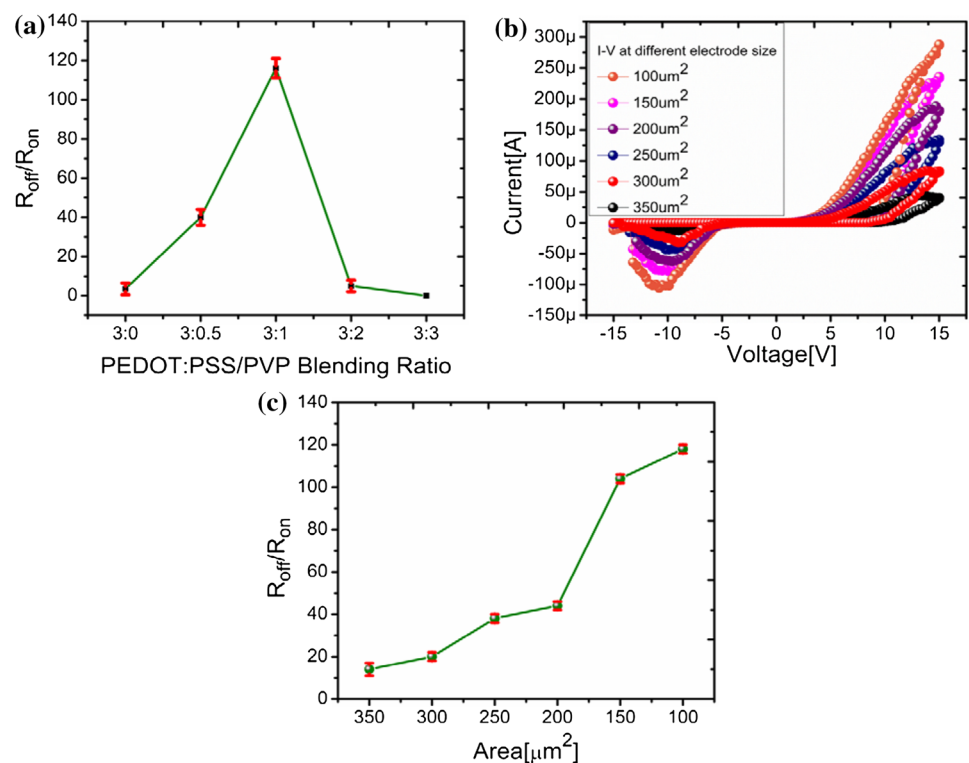
PEDOT:PSS-based device also did not shown memory effect, as shown in Fig. 2b.

However, we demonstrate that the heterojunction of these two layers can achieve the resistive switching characteristics. Hence, we fabricate the device based on heterojunction of methyl red and PEDOT:PSS. The device was biased with a double voltage sweep from  $-10$  to  $10$  V with a current compliance of  $100$  mA, a resistive switching behavior was observed with two different resistive states LRS and HRS, as shown in Fig. 2c. The resistance of the HRS state was observed to be  $6.5$  k $\Omega$  and that of the LRS is  $1$  k $\Omega$ . The device exhibited endurance cycles more than  $200$  cycles that confirms the device stability against endurance. It shows insensitivity by the endurance cycles that almost symmetric I–V curves (the current goes to  $10$  mA on negative side and the current goes to  $8$  mA on positive side) are obtained. Due to charge transition in heterojunction for this stable and exact bipolar behavior, the conducting channels on the interface of both layers of the proposed device are generated for LRS, and the conducting paths are dissolved for HRS [18, 24, 25]. To verify the consistency of the proposed device, we fabricated five devices of  $2 \times 2$  crossbar memory and measured the IV behavior, as shown on semi-log scale in Fig. 2d. They showed stable fabrication consistency, since they have small switching voltage variation in between  $\pm 8$  and  $\pm 8.02$  V.

From these results, we came to know that the  $R_{\text{off}}/R_{\text{on}}$  ratio is low which is just  $6.5$  and need to be improve as it

is important in resistive switching for memory application with good detection margin. To increase the  $R_{\text{off}}/R_{\text{on}}$  ratio, the heterojunction materials should possess a high resistivity to achieve high resistance. Methyl red is an organic semiconductor with a high bandgap above  $3.2$  eV, whereas the PEDOT:PSS is an organic conducting polymer. Therefore, we added PVP into the PEDOT:PSS solution to increase its resistivity, where the PVP is an insulator polymer. The PDEOT:PSS and the PVP were blended with various mixing ratio, as shown in Fig. 3a, and the optimum blending ratio was found to be  $3:1$  for maximum resistive switched  $R_{\text{off}}/R_{\text{on}}$  ratio. By increasing the PVP in the PEDOT:PSS from the blending ratio  $3:0$ , HRS of composite material was dominantly increased, and hence, the  $R_{\text{off}}/R_{\text{on}}$  ratio is increased maximum at  $3:1$ . However, the  $R_{\text{off}}/R_{\text{on}}$  ratio is reduced again due to LRS of composite material was dominantly increased over the blending ratio,  $3:1$ . Using this optimum ratio of  $3:1$ , we obtained the  $R_{\text{off}}/R_{\text{on}}$  ratio of  $121$ , which is increased  $19$  times than before the device. To increase the  $R_{\text{off}}/R_{\text{on}}$  ratio using dependency on device size, we have fabricated devices with different active area sizes controlled through crossbar electrodes. At the blending ratio  $3:0$ ,  $3:0.5$ ,  $3:1$ ,  $3:2$ , and  $3:3$  on the  $100$   $\mu\text{m}^2$  sandwiched area in Fig. 3a, their mean values and variations obtained by measuring five samples for each rat are  $(3.5, 40, 116, 5, 0)$  and  $(\pm 3, \pm 4, \pm 5, \pm 3, \pm 0)$ , respectively. Figure 3b shows the I–V curves of different sandwiched areas for different  $R_{\text{off}}/R_{\text{on}}$  ratios. At the blending ratio of  $3:1$ ,

**Fig. 3** **a** The  $R_{\text{off}}/R_{\text{on}}$  ratio at different blending ratio for the PEDOT:PSS and PVP composite on the  $100$   $\mu\text{m}^2$  sandwiched area. **b** I–V curves of the different sandwiched active areas between *top* and *bottom* electrodes at the blending ratio of  $3:1$ . **c** The  $R_{\text{off}}/R_{\text{on}}$  ratio graph on different active sandwiched areas between *top* and *bottom* electrodes (device size). The  $R_{\text{off}}/R_{\text{on}}$  ratio is inversely proportional to the device size and the blending ratio is  $3:1$

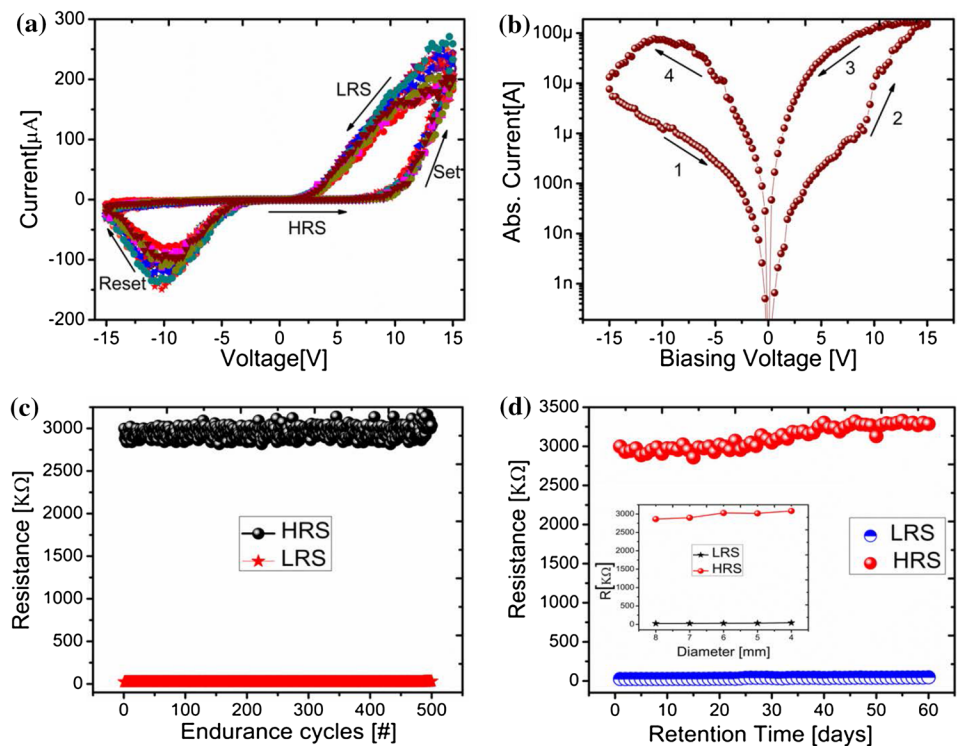


we found that  $R_{\text{off}}/R_{\text{on}}$  ratio is inversely proportional to the device size, as shown in Fig. 3c. Starting from  $100 \mu\text{m}^2$  area as a limitation of our e-printing system, the  $R_{\text{off}}/R_{\text{on}}$  ratio was observed to be 121, and as the active area was increased, the  $R_{\text{off}}/R_{\text{on}}$  ratio was decreased to 14, as shown in Fig. 3c. From this analysis, we observed that in a small sandwiched active area between the top and bottom electrodes, the  $R_{\text{off}}/R_{\text{on}}$  ratio is high and vice versa. As we observed that resistive switching behavior has dependence on size of electrode, so the resistive switching mechanism of our device is charge transaction based not filamentary based [23]. To get the mean values and their variations for the areas (100, 150, 200, 250, 300, and  $350 \mu\text{m}^2$ ), six samples for each area are measured, where the obtained mean values of  $R_{\text{off}}/R_{\text{on}}$  ratio are (118, 104, 44, 38, 20, and 14) and the variations are ( $\pm 3$ ,  $\pm 2$ ,  $\pm 2$ ,  $\pm 2$ , and  $\pm 2$ ).

Using the blending ratio of 3:1 and the area of  $100 \mu\text{m}^2$ , we fabricated the PEDOT:PSS/PVP composite and methyl red heterojunction device, and the device was biased with a double voltage sweep from  $-15 \text{ V}$  to  $15 \text{ V}$  with a current compliance of  $10 \text{ mA}$ . I–V curves of the device with two different states LRS ( $24.7 \text{ k}\Omega$ ) and HRS ( $3000 \text{ k}\Omega$ ) along hundreds of endurance cycles were measured as shown in Fig. 4a. The device  $R_{\text{off}}/R_{\text{on}}$  ratio was increased from 6.5 to 121. However, the threshold voltage was also increased from  $\pm 8.02 \text{ V}$  to  $\pm 10.2 \text{ V}$ . The threshold voltage is increased because of PVP material blended in PEDOT:PSS. The reset of memristor occurred around  $-10.2 \text{ V}$  and the set occurred around  $+10.2 \text{ V}$ . During the voltage sweep from

$-15 \text{ V}$  to  $15 \text{ V}$ , the device did not go in saturation as evident in the Fig. 4a. Figure 4b shows the absolute current voltage graph of the devices on semi-log scale which indicates that the devices exhibit bipolar resistive switching as their currents pass through  $0 \text{ V}$ . Resistive state of the device is starting from “1” (HRS) followed by “2” which is transition from HRS to LRS, then voltage sweep goes back and passes through “3” which is LRS state, and at  $-10.2 \text{ V}$ , it goes again to HRS through “4” and complete the resistive switching cycle. As shown in Fig. 4c, the endurance test of the fabricated resistive switch was checked for 500 biasing cycles. The maximum resistance variation in LRS and HRS is  $52 \Omega$  and  $498 \Omega$ , respectively, which shows that the LRS is more stable than the HRS. In terms of endurance cycles and retention time, the performance of the proposed heterojunction-based resistive switching device is improved as compared to previous heterojunction resistive devices [16, 17]. The switching voltages to the HRS and the LRS are  $\pm 10.2 \text{ V}$ , and the non-volatility of the proposed device was also measured for more than 60 days, as shown in Fig. 4d, and a small change occurred in HRS and LRS resistance states that the device shows a stable and non-volatile characteristics. Here, although the resistance drift occurs in both resistive states, HRS and LRS, the  $R_{\text{off}}/R_{\text{on}}$  ratio was not affected much. The mechanical characteristics were analyzed by bending it on different diameters from flat down to  $4 \text{ mm}$  diameter using homemade bending machine, as shown in the inset of Fig. 4d. It was found that minimum bending diameter was  $4 \text{ mm}$ , bending beyond

**Fig. 4** Characterizations of the improved proposed resistive switching device using best blending ratio and device size, **a** I–V curve endurance cycles of the PEDOT:PSS/PVP composite and methyl red heterojunction, **b** absolute current–voltage analysis on semi-log scale, **c** HRS and LRS state of resistive switch for 500 endurance cycles, and **d** retention time analysis and the inset figure shows bending test down to  $4 \text{ mm}$



4 mm the device got opened circuited due to the breakage of active layers.

## 4 Conclusion

Using the printed techniques, we have proposed a novel resistive switching device based on PEDOT:PSS/PVP composite and methyl red heterojunction for the first time. The top and bottom electrodes of the proposed device were fabricated on the flexible PET substrate through the Dimatix material printer DMP-3000 at ambient conditions, and the PEDOT:PSS/PVP composite layer and methyl red layers were fabricated through the spin coater at 3000 rpm. Morphological characterizations were carried out with the help of FE-SEM, and observed uniformly deposition. The device exhibited resistive switching at dual polarity voltage of  $\pm 10.2$  V, and the OFF and ON state resistances were found to be 3000 k $\Omega$  and 24.7 k $\Omega$ , respectively. The  $R_{\text{off}}/R_{\text{on}}$  ratio could be designed from 6.5 to 121 by blending PVP into PEDOT:PSS and adjusting an active area. The device has exhibited flexibility down to 4 mm diameter and the retention time was recorded to be over 60 days.

**Acknowledgements** This work was supported by the National Research Foundation of Korea (NRF) Grant funded by the Korea government (MSIP) (NRF-2016R1A2B4015627).

## References

1. L. Chua, Appl. Phys. A **102**, 765 (2011)
2. D.B. Strukov, G.S. Snider, D.R. Stewart, R.S. Williams, Nature **453**, 80 (2008)
3. S. Ali, J. Bae, K.H. Choi, C.H. Lee, Y.H. Doh, S. Shin, N.P. Kobayashi, Org. Electron **17**, 121 (2015)
4. W. Shih, J. Zhou, H.-J. Qiu, S. Yang, Z.Mi Che, I. Shih, Nanotechnology **21**, 125201 (2010)
5. S. Ali, J. Bae, C.H. Lee, K.H. Choi, Y.H. Doh, Org. Electron **25**, 225 (2015)
6. F.C. Chen, C.W. Chu, J. He, Y. Yang, Appl. Phys. Lett. **85**, 3295 (2006)
7. K. Szot, W. Speier, G. Bihlmayer, R. Waser, Nat. Mater. **5**, 312 (2006)
8. C. Quinteros, R. Zazpe, F.G. Marlasca, F. Golmar, F. Casanova, P. Stoliar, L. Hueso, P. Levy, J. Appl. Phys. **115**, 024501 (2014)
9. J.-k. Li, C. Ma, K.-J. Jin, C. Ge, L. Gu, X. He, W.-J. Zhou, Q.-H. Zhang, H.-B. Lu, G.-Z. Yang, Appl. Phys. Lett. **108**, 242901 (2016)
10. J.J.T. Wagenaar, M. Morales-Masis, J.M. van Ruitenbeek, J. Appl. Phys **111**, 014302 (2012)
11. X.Y. Yang, S.B. Long, K.W. Zhang, X.Y. Liu, G.M. Wang, X.J. Lian, Q. Liu, H.B. Lv, M. Wang, H.W. Xie, H.T. Sun, P.X. Sun, J. Sune, M. Liu, J. Phys. D Appl. Phys. **46**, 245107 (2013)
12. C. Schindler, S.C.P. Thernadam, R. Waser, M.N. Kozicki, IEEE Trans. Electron Devices **54**, 2762 (2007)
13. Y. Li, Y. P. Zhong, L. Xu, J.J. Zhang, X.H. Xu, H.J. Sun, X.S. Miao, Sci. Rep. **3**, 1619 (2013)
14. K.H. Choi, J. Ali, Y.H. Doh, Jpn. J. Appl. Phys. **54**, 035103 (2015)
15. J.J. Yang, M.X. Zhang, M.D. Pickett, F. Miao, J.P. Strachan, W.D. Li, W. Yi, D.A. Ohlberg, B.J. Choi, W. Wu, J.H. Nickel, Appl. Phys. Lett. **11**, 113501 (2012)
16. Y. Jo, B.U.J. Kim, D. Kim, H. Woo, I. Kim, W. Park, H. Im, H. Kim, J Korean Phys. Soc. **64**, 173 (2014)
17. Z. Fan, X. Fan, A. Le, L. Dong, 12th IEEE international Conference on Nanotechnology (IEEE-NANO), **1** (2012)
18. Q.D. Ling, D.J. Liawb, C. Zhuc, D.S.H. Chanc, E.T. Kanga, K.G. Neoha, Prog. Polym. Sci. **33**, 917 (2008)
19. Y.C. Chen, H.C. Yu, C.Y. Huang, W.L. Chung, S.L. Wu, Y.K. Su, Nature **5**, 10022 (2015)
20. N. Fuentes, A.M. Lasanta, L.A.D. Cienfuegos, M. Ribagorda, A. Parra, J.M. Cuerva, Nanoscale **3**, 4003 (2011)
21. B. Cho, S. Song, Y. Ji, T. T.W. Kim, T. Lee, Adv. Funct. Mater. **21**, 2806 (2011)
22. S. Choi, S.H. Hong, S.H. Cho, S. Park, S.M. Park, O. Kim, M. Ree, Adv. Mater **20**, 1766 (2008)
23. H.Y. Peng, G.P. Li, J.Y. Ye, Z.P. Wei, Z. Zhang, D.D. Wang, G.Z. Xing, T. Wu, Appl. Phys. Lett. **96**, 192113 (2010)
24. J.-K. Choi, J.-H. Kim, S.-H. Kim, D.H. Suh, Appl. Phys. Lett. **89**, 15 (2006)
25. S. Miao, Y. Zhu, Q. Bao, H. Li, N. Li, S. Ji, Q. Xu, J. Lu, L. Wang, J. Phys. Chem. C **118**(4), 2154–2160 (2014)